

Search for Lepton-Flavor and Lepton-Number Violation in the Decay $\tau^- \rightarrow \ell^\mp h^\pm h^\mp$

- B. Aubert,¹ R. Barate,¹ D. Boutigny,¹ F. Couderc,¹ Y. Karyotakis,¹ J. P. Lees,¹ V. Poireau,¹ V. Tisserand,¹
A. Zghiche,¹ E. Grauges,² A. Palano,³ M. Pappagallo,³ A. Pompili,³ J. C. Chen,⁴ N. D. Qi,⁴ G. Rong,⁴ P. Wang,⁴
Y. S. Zhu,⁴ G. Eigen,⁵ I. Ofte,⁵ B. Stugu,⁵ G. S. Abrams,⁶ M. Battaglia,⁶ A. B. Breon,⁶ D. N. Brown,⁶
J. Button-Shafer,⁶ R. N. Cahn,⁶ E. Charles,⁶ C. T. Day,⁶ M. S. Gill,⁶ A. V. Gritsan,⁶ Y. Groysman,⁶
R. G. Jacobsen,⁶ R. W. Kadel,⁶ J. Kadyk,⁶ L. T. Kerth,⁶ Yu. G. Kolomensky,⁶ G. Kukartsev,⁶ G. Lynch,⁶
L. M. Mir,⁶ P. J. Oddone,⁶ T. J. Orimoto,⁶ M. Pripstein,⁶ N. A. Roe,⁶ M. T. Ronan,⁶ W. A. Wenzel,⁶ M. Barrett,⁷
K. E. Ford,⁷ T. J. Harrison,⁷ A. J. Hart,⁷ C. M. Hawkes,⁷ S. E. Morgan,⁷ A. T. Watson,⁷ M. Fritsch,⁸ K. Goetzen,⁸
T. Held,⁸ H. Koch,⁸ B. Lewandowski,⁸ M. Pelizaeus,⁸ K. Peters,⁸ T. Schroeder,⁸ M. Steinke,⁸ J. T. Boyd,⁹
J. P. Burke,⁹ N. Chevalier,⁹ W. N. Cottingham,⁹ M. P. Kelly,⁹ T. Cuhadar-Donszelmann,¹⁰ B. G. Fulsom,¹⁰
C. Hearty,¹⁰ N. S. Knecht,¹⁰ T. S. Mattison,¹⁰ J. A. McKenna,¹⁰ A. Khan,¹¹ P. Kyberd,¹¹ M. Saleem,¹¹
L. Teodorescu,¹¹ A. E. Blinov,¹² V. E. Blinov,¹² A. D. Bukan,¹² V. P. Druzhinin,¹² V. B. Golubev,¹²
E. A. Kravchenko,¹² A. P. Onuchin,¹² S. I. Serednyakov,¹² Yu. I. Skovpen,¹² E. P. Solodov,¹² A. N. Yushkov,¹²
D. Best,¹³ M. Bondioli,¹³ M. Bruinsma,¹³ M. Chao,¹³ I. Eschrich,¹³ D. Kirkby,¹³ A. J. Lankford,¹³
M. Mandelkern,¹³ R. K. Mommsen,¹³ W. Roethel,¹³ D. P. Stoker,¹³ C. Buchanan,¹⁴ B. L. Hartfiel,¹⁴
A. J. R. Weinstein,¹⁴ S. D. Foulkes,¹⁵ J. W. Gary,¹⁵ O. Long,¹⁵ B. C. Shen,¹⁵ K. Wang,¹⁵ L. Zhang,¹⁵ D. del Re,¹⁶
H. K. Hadavand,¹⁶ E. J. Hill,¹⁶ D. B. MacFarlane,¹⁶ H. P. Paar,¹⁶ S. Rahatlou,¹⁶ V. Sharma,¹⁶ J. W. Berryhill,¹⁷
C. Campagnari,¹⁷ A. Cunha,¹⁷ B. Dahmes,¹⁷ T. M. Hong,¹⁷ M. A. Mazur,¹⁷ J. D. Richman,¹⁷ W. Verkerke,¹⁷
T. W. Beck,¹⁸ A. M. Eisner,¹⁸ C. J. Flacco,¹⁸ C. A. Heusch,¹⁸ J. Kroeseberg,¹⁸ W. S. Lockman,¹⁸ G. Nesom,¹⁸
T. Schalk,¹⁸ B. A. Schumm,¹⁸ A. Seiden,¹⁸ P. Spradlin,¹⁸ D. C. Williams,¹⁸ M. G. Wilson,¹⁸ J. Albert,¹⁹
E. Chen,¹⁹ G. P. Dubois-Felsmann,¹⁹ A. Dvoretskii,¹⁹ D. G. Hitlin,¹⁹ I. Narsky,¹⁹ T. Piatenko,¹⁹ F. C. Porter,¹⁹
A. Ryd,¹⁹ A. Samuel,¹⁹ R. Andreassen,²⁰ S. Jayatilleke,²⁰ G. Mancinelli,²⁰ B. T. Meadows,²⁰ M. D. Sokoloff,²⁰
F. Blanc,²¹ P. Bloom,²¹ S. Chen,²¹ W. T. Ford,²¹ U. Nauenberg,²¹ A. Olivas,²¹ P. Rankin,²¹ W. O. Ruddick,²¹
J. G. Smith,²¹ K. A. Ulmer,²¹ S. R. Wagner,²¹ J. Zhang,²¹ A. Chen,²² E. A. Eckhart,²² A. Soffer,²² W. H. Toki,²²
R. J. Wilson,²² Q. Zeng,²² D. Altenburg,²³ E. Feltresi,²³ A. Hauke,²³ B. Spaan,²³ T. Brandt,²⁴ J. Brose,²⁴
M. Dickopp,²⁴ V. Klose,²⁴ H. M. Lacker,²⁴ R. Nogowski,²⁴ S. Otto,²⁴ A. Petzold,²⁴ G. Schott,²⁴ J. Schubert,²⁴
K. R. Schubert,²⁴ R. Schwierz,²⁴ J. E. Sundermann,²⁴ D. Bernard,²⁵ G. R. Bonneau,²⁵ P. Grenier,²⁵ S. Schrenk,²⁵
Ch. Thiebaut,²⁵ G. Vasileiadis,²⁵ M. Verderi,²⁵ D. J. Bard,²⁶ P. J. Clark,²⁶ W. Gradl,²⁶ F. Muheim,²⁶ S. Playfer,²⁶
Y. Xie,²⁶ M. Andreotti,²⁷ V. Azzolini,²⁷ D. Bettoni,²⁷ C. Bozzi,²⁷ R. Calabrese,²⁷ G. Cibinetto,²⁷ E. Luppi,²⁷
M. Negrini,²⁷ L. Piemontese,²⁷ F. Anulli,²⁸ R. Baldini-Ferroli,²⁸ A. Calcaterra,²⁸ R. de Sangro,²⁸ G. Finocchiaro,²⁸
P. Patteri,²⁸ I. M. Peruzzi,²⁸, * M. Piccolo,²⁸ A. Zallo,²⁸ A. Buzzo,²⁹ R. Capra,²⁹ R. Contri,²⁹ M. Lo Vetere,²⁹
M. Macri,²⁹ M. R. Monge,²⁹ S. Passaggio,²⁹ C. Patrignani,²⁹ E. Robutti,²⁹ A. Santroni,²⁹ S. Tosi,²⁹ S. Bailey,³⁰
G. Brandenburg,³⁰ K. S. Chaisanguanthum,³⁰ M. Morii,³⁰ E. Won,³⁰ J. Wu,³⁰ R. S. Dubitzky,³¹ U. Langenegger,³¹
J. Marks,³¹ S. Schenk,³¹ U. Uwer,³¹ W. Bhimji,³² D. A. Bowerman,³² P. D. Dauncey,³² U. Egede,³² R. L. Flack,³²
J. R. Gaillard,³² G. W. Morton,³² J. A. Nash,³² M. B. Nikolich,³² G. P. Taylor,³² W. P. Vazquez,³² M. J. Charles,³³
W. F. Mader,³³ U. Mallik,³³ A. K. Mohapatra,³³ J. Cochran,³⁴ H. B. Crawley,³⁴ V. Eges,³⁴ W. T. Meyer,³⁴
S. Prell,³⁴ E. I. Rosenberg,³⁴ A. E. Rubin,³⁴ J. Yi,³⁴ N. Arnaud,³⁵ M. Davier,³⁵ X. Giroux,³⁵ G. Grosdidier,³⁵
A. Höcker,³⁵ F. Le Diberder,³⁵ V. Lepeltier,³⁵ A. M. Lutz,³⁵ A. Oyanguren,³⁵ T. C. Petersen,³⁵ M. Pierini,³⁵
S. Plaszczynski,³⁵ S. Rodier,³⁵ P. Roudeau,³⁵ M. H. Schune,³⁵ A. Stocchi,³⁵ G. Wormser,³⁵ C. H. Cheng,³⁶
D. J. Lange,³⁶ M. C. Simani,³⁶ D. M. Wright,³⁶ A. J. Bevan,³⁷ C. A. Chavez,³⁷ J. P. Coleman,³⁷ I. J. Forster,³⁷
J. R. Fry,³⁷ E. Gabathuler,³⁷ R. Gamet,³⁷ K. A. George,³⁷ D. E. Hutchcroft,³⁷ R. J. Parry,³⁷ D. J. Payne,³⁷
K. C. Schofield,³⁷ C. Touramanis,³⁷ C. M. Cormack,³⁸ F. Di Lodovico,³⁸ R. Sacco,³⁸ C. L. Brown,³⁹ G. Cowan,³⁹
H. U. Flaecher,³⁹ M. G. Green,³⁹ D. A. Hopkins,³⁹ P. S. Jackson,³⁹ T. R. McMahon,³⁹ S. Ricciardi,³⁹ F. Salvatore,³⁹
D. Brown,⁴⁰ C. L. Davis,⁴⁰ J. Allison,⁴¹ N. R. Barlow,⁴¹ R. J. Barlow,⁴¹ M. C. Hodgkinson,⁴¹ G. D. Lafferty,⁴¹
M. T. Naisbit,⁴¹ J. C. Williams,⁴¹ C. Chen,⁴² A. Farbin,⁴² W. D. Hulsbergen,⁴² A. Jawahery,⁴² D. Kovalskyi,⁴²
C. K. Lae,⁴² V. Lillard,⁴² D. A. Roberts,⁴² G. Simi,⁴² G. Blaylock,⁴³ C. Dallapiccola,⁴³ S. S. Hertzbach,⁴³
R. Kofler,⁴³ V. B. Koptchev,⁴³ X. Li,⁴³ T. B. Moore,⁴³ S. Saremi,⁴³ H. Staengle,⁴³ S. Willocq,⁴³ R. Cowan,⁴⁴
K. Koeneke,⁴⁴ G. Sciolla,⁴⁴ S. J. Sekula,⁴⁴ M. Spitznagel,⁴⁴ F. Taylor,⁴⁴ R. K. Yamamoto,⁴⁴ H. Kim,⁴⁵ P. M. Patel,⁴⁵
S. H. Robertson,⁴⁵ A. Lazzaro,⁴⁶ V. Lombardo,⁴⁶ F. Palombo,⁴⁶ J. M. Bauer,⁴⁷ L. Cremaldi,⁴⁷ V. Eschenburg,⁴⁷
R. Godang,⁴⁷ R. Kroeger,⁴⁷ J. Reidy,⁴⁷ D. A. Sanders,⁴⁷ D. J. Summers,⁴⁷ H. W. Zhao,⁴⁷ S. Brunet,⁴⁸ D. Côté,⁴⁸

P. Taras,⁴⁸ B. Viaud,⁴⁸ H. Nicholson,⁴⁹ N. Cavallo,⁵⁰, † G. De Nardo,⁵⁰ F. Fabozzi,⁵⁰, † C. Gatto,⁵⁰ L. Lista,⁵⁰ D. Monorchio,⁵⁰ P. Paolucci,⁵⁰ D. Piccolo,⁵⁰ C. Sciacca,⁵⁰ M. Baak,⁵¹ H. Bulten,⁵¹ G. Raven,⁵¹ H. L. Snoek,⁵¹ L. Welden,⁵¹ C. P. Jessop,⁵² J. M. LoSecco,⁵² T. Allmendinger,⁵³ G. Benelli,⁵³ K. K. Gan,⁵³ K. Honscheid,⁵³ D. Hufnagel,⁵³ P. D. Jackson,⁵³ H. Kagan,⁵³ R. Kass,⁵³ T. Pulliam,⁵³ A. M. Rahimi,⁵³ R. Ter-Antonyan,⁵³ Q. K. Wong,⁵³ J. Brau,⁵⁴ R. Frey,⁵⁴ O. Igonkina,⁵⁴ M. Lu,⁵⁴ C. T. Potter,⁵⁴ N. B. Sinev,⁵⁴ D. Strom,⁵⁴ J. Strube,⁵⁴ E. Torrence,⁵⁴ A. Dorigo,⁵⁵ F. Galeazzi,⁵⁵ M. Margoni,⁵⁵ M. Morandin,⁵⁵ M. Posocco,⁵⁵ M. Rotondo,⁵⁵ F. Simonetto,⁵⁵ R. Stroili,⁵⁵ C. Voci,⁵⁵ M. Benayoun,⁵⁶ H. Briand,⁵⁶ J. Chauveau,⁵⁶ P. David,⁵⁶ L. Del Buono,⁵⁶ Ch. de la Vaissière,⁵⁶ O. Hamon,⁵⁶ M. J. J. John,⁵⁶ Ph. Leruste,⁵⁶ J. Malclès,⁵⁶ J. Ocariz,⁵⁶ L. Roos,⁵⁶ G. Therin,⁵⁶ P. K. Behera,⁵⁷ L. Gladney,⁵⁷ Q. H. Guo,⁵⁷ J. Panetta,⁵⁷ M. Biasini,⁵⁸ R. Covarelli,⁵⁸ S. Pacetti,⁵⁸ M. Pioppi,⁵⁸ C. Angelini,⁵⁹ G. Batignani,⁵⁹ S. Bettarini,⁵⁹ F. Bucci,⁵⁹ G. Calderini,⁵⁹ M. Carpinelli,⁵⁹ R. Cenci,⁵⁹ F. Forti,⁵⁹ M. A. Giorgi,⁵⁹ A. Lusiani,⁵⁹ G. Marchiori,⁵⁹ M. Morganti,⁵⁹ N. Neri,⁵⁹ E. Paoloni,⁵⁹ M. Rama,⁵⁹ G. Rizzo,⁵⁹ J. Walsh,⁵⁹ M. Haire,⁶⁰ D. Judd,⁶⁰ D. E. Wagoner,⁶⁰ J. Biesiada,⁶¹ N. Danielson,⁶¹ P. Elmer,⁶¹ Y. P. Lau,⁶¹ C. Lu,⁶¹ J. Olsen,⁶¹ A. J. S. Smith,⁶¹ A. V. Telnov,⁶¹ F. Bellini,⁶² G. Cavoto,⁶² A. D'Orazio,⁶² E. Di Marco,⁶² R. Faccini,⁶² F. Ferrarotto,⁶² F. Ferroni,⁶² M. Gaspero,⁶² L. Li Gioi,⁶² M. A. Mazzoni,⁶² S. Morganti,⁶² G. Piredda,⁶² F. Polci,⁶² F. Safai Tehrani,⁶² C. Voena,⁶² H. Schröder,⁶³ G. Wagner,⁶³ R. Waldi,⁶³ T. Adye,⁶⁴ N. De Groot,⁶⁴ B. Franek,⁶⁴ G. P. Gopal,⁶⁴ E. O. Olaiya,⁶⁴ F. F. Wilson,⁶⁴ R. Aleksan,⁶⁵ S. Emery,⁶⁵ A. Gaidot,⁶⁵ S. F. Ganzhur,⁶⁵ P.-F. Giraud,⁶⁵ G. Graziani,⁶⁵ G. Hamel de Monchenault,⁶⁵ W. Kozanecki,⁶⁵ M. Legendre,⁶⁵ G. W. London,⁶⁵ B. Mayer,⁶⁵ G. Vasseur,⁶⁵ Ch. Yèche,⁶⁵ M. Zito,⁶⁵ M. V. Purohit,⁶⁶ A. W. Weidemann,⁶⁶ J. R. Wilson,⁶⁶ F. X. Yumiceva,⁶⁶ T. Abe,⁶⁷ M. T. Allen,⁶⁷ D. Aston,⁶⁷ R. Bartoldus,⁶⁷ N. Berger,⁶⁷ A. M. Boyarski,⁶⁷ O. L. Buchmueller,⁶⁷ R. Claus,⁶⁷ M. R. Convery,⁶⁷ M. Cristinziani,⁶⁷ J. C. Dingfelder,⁶⁷ D. Dong,⁶⁷ J. Dorfan,⁶⁷ D. Dujmic,⁶⁷ W. Dunwoodie,⁶⁷ S. Fan,⁶⁷ R. C. Field,⁶⁷ T. Glanzman,⁶⁷ S. J. Gowdy,⁶⁷ T. Hadig,⁶⁷ V. Halyo,⁶⁷ C. Hast,⁶⁷ T. Hryna'ova,⁶⁷ W. R. Innes,⁶⁷ M. H. Kelsey,⁶⁷ P. Kim,⁶⁷ M. L. Kocian,⁶⁷ D. W. G. S. Leith,⁶⁷ J. Libby,⁶⁷ S. Luitz,⁶⁷ V. Luth,⁶⁷ H. L. Lynch,⁶⁷ H. Marsiske,⁶⁷ R. Messner,⁶⁷ D. R. Muller,⁶⁷ C. P. O'Grady,⁶⁷ V. E. Ozcan,⁶⁷ A. Perazzo,⁶⁷ M. Perl,⁶⁷ B. N. Ratcliff,⁶⁷ A. Roodman,⁶⁷ A. A. Salnikov,⁶⁷ R. H. Schindler,⁶⁷ J. Schwiening,⁶⁷ A. Snyder,⁶⁷ J. Stelzer,⁶⁷ D. Su,⁶⁷ M. K. Sullivan,⁶⁷ K. Suzuki,⁶⁷ S. Swain,⁶⁷ J. M. Thompson,⁶⁷ J. Va'vra,⁶⁷ M. Weaver,⁶⁷ W. J. Wisniewski,⁶⁷ M. Wittgen,⁶⁷ D. H. Wright,⁶⁷ A. K. Yarritu,⁶⁷ K. Yi,⁶⁷ C. C. Young,⁶⁷ P. R. Burchat,⁶⁸ A. J. Edwards,⁶⁸ S. A. Majewski,⁶⁸ B. A. Petersen,⁶⁸ C. Roat,⁶⁸ M. Ahmed,⁶⁹ S. Ahmed,⁶⁹ M. S. Alam,⁶⁹ J. A. Ernst,⁶⁹ M. A. Saeed,⁶⁹ F. R. Wappler,⁶⁹ S. B. Zain,⁶⁹ W. Bugg,⁷⁰ M. Krishnamurthy,⁷⁰ S. M. Spanier,⁷⁰ R. Eckmann,⁷¹ J. L. Ritchie,⁷¹ A. Satpathy,⁷¹ R. F. Schwitters,⁷¹ J. M. Izen,⁷² I. Kitayama,⁷² X. C. Lou,⁷² S. Ye,⁷² F. Bianchi,⁷³ M. Bona,⁷³ F. Gallo,⁷³ D. Gamba,⁷³ M. Bomben,⁷⁴ L. Bosisio,⁷⁴ C. Cartaro,⁷⁴ F. Cossutti,⁷⁴ G. Della Ricca,⁷⁴ S. Dittongo,⁷⁴ S. Grancagnolo,⁷⁴ L. Lanceri,⁷⁴ L. Vitale,⁷⁴ F. Martinez-Vidal,⁷⁵ R. S. Panvini,⁷⁶, † Sw. Banerjee,⁷⁷ B. Bhuyan,⁷⁷ C. M. Brown,⁷⁷ D. Fortin,⁷⁷ K. Hamano,⁷⁷ R. Kowalewski,⁷⁷ J. M. Roney,⁷⁷ R. J. Sobie,⁷⁷ J. J. Back,⁷⁸ P. F. Harrison,⁷⁸ T. E. Latham,⁷⁸ G. B. Mohanty,⁷⁸ H. R. Band,⁷⁹ X. Chen,⁷⁹ B. Cheng,⁷⁹ S. Dasu,⁷⁹ M. Datta,⁷⁹ A. M. Eichenbaum,⁷⁹ K. T. Flood,⁷⁹ M. Graham,⁷⁹ J. J. Hollar,⁷⁹ J. R. Johnson,⁷⁹ P. E. Kutter,⁷⁹ H. Li,⁷⁹ R. Liu,⁷⁹ B. Mellado,⁷⁹ A. Mihalyi,⁷⁹ Y. Pan,⁷⁹ R. Prepost,⁷⁹ P. Tan,⁷⁹ J. H. von Wimmersperg-Toeller,⁷⁹ S. L. Wu,⁷⁹ Z. Yu,⁷⁹ and H. Neal⁸⁰

(The BABAR Collaboration)

¹Laboratoire de Physique des Particules, F-74941 Annecy-le-Vieux, France

²IFAE, Universitat Autònoma de Barcelona, E-08193 Bellaterra, Barcelona, Spain

³Università di Bari, Dipartimento di Fisica and INFN, I-70126 Bari, Italy

⁴Institute of High Energy Physics, Beijing 100039, China

⁵University of Bergen, Inst. of Physics, N-5007 Bergen, Norway

⁶Lawrence Berkeley National Laboratory and University of California, Berkeley, California 94720, USA

⁷University of Birmingham, Birmingham, B15 2TT, United Kingdom

⁸Ruhr Universität Bochum, Institut für Experimentalphysik 1, D-44780 Bochum, Germany

⁹University of Bristol, Bristol BS8 1TL, United Kingdom

¹⁰University of British Columbia, Vancouver, British Columbia, Canada V6T 1Z1

¹¹Brunel University, Uxbridge, Middlesex UB8 3PH, United Kingdom

¹²Budker Institute of Nuclear Physics, Novosibirsk 630090, Russia

¹³University of California at Irvine, Irvine, California 92697, USA

¹⁴University of California at Los Angeles, Los Angeles, California 90024, USA

¹⁵University of California at Riverside, Riverside, California 92521, USA

¹⁶University of California at San Diego, La Jolla, California 92093, USA

¹⁷University of California at Santa Barbara, Santa Barbara, California 93106, USA

¹⁸University of California at Santa Cruz, Institute for Particle Physics, Santa Cruz, California 95064, USA

- ¹⁹California Institute of Technology, Pasadena, California 91125, USA
²⁰University of Cincinnati, Cincinnati, Ohio 45221, USA
²¹University of Colorado, Boulder, Colorado 80309, USA
²²Colorado State University, Fort Collins, Colorado 80523, USA
²³Universität Dortmund, Institut für Physik, D-44221 Dortmund, Germany
²⁴Technische Universität Dresden, Institut für Kern- und Teilchenphysik, D-01062 Dresden, Germany
²⁵Ecole Polytechnique, LLR, F-91128 Palaiseau, France
²⁶University of Edinburgh, Edinburgh EH9 3JZ, United Kingdom
²⁷Università di Ferrara, Dipartimento di Fisica and INFN, I-44100 Ferrara, Italy
²⁸Laboratori Nazionali di Frascati dell'INFN, I-00044 Frascati, Italy
²⁹Università di Genova, Dipartimento di Fisica and INFN, I-16146 Genova, Italy
³⁰Harvard University, Cambridge, Massachusetts 02138, USA
³¹Universität Heidelberg, Physikalisches Institut, Philosophenweg 12, D-69120 Heidelberg, Germany
³²Imperial College London, London, SW7 2AZ, United Kingdom
³³University of Iowa, Iowa City, Iowa 52242, USA
³⁴Iowa State University, Ames, Iowa 50011-3160, USA
³⁵Laboratoire de l'Accélérateur Linéaire, F-91898 Orsay, France
³⁶Lawrence Livermore National Laboratory, Livermore, California 94550, USA
³⁷University of Liverpool, Liverpool L69 7ZE, United Kingdom
³⁸Queen Mary, University of London, E1 4NS, United Kingdom
³⁹University of London, Royal Holloway and Bedford New College, Egham, Surrey TW20 0EX, United Kingdom
⁴⁰University of Louisville, Louisville, Kentucky 40292, USA
⁴¹University of Manchester, Manchester M13 9PL, United Kingdom
⁴²University of Maryland, College Park, Maryland 20742, USA
⁴³University of Massachusetts, Amherst, Massachusetts 01003, USA
⁴⁴Massachusetts Institute of Technology, Laboratory for Nuclear Science, Cambridge, Massachusetts 02139, USA
⁴⁵McGill University, Montréal, Québec, Canada H3A 2T8
⁴⁶Università di Milano, Dipartimento di Fisica and INFN, I-20133 Milano, Italy
⁴⁷University of Mississippi, University, Mississippi 38677, USA
⁴⁸Université de Montréal, Laboratoire René J. A. Lévesque, Montréal, Québec, Canada H3C 3J7
⁴⁹Mount Holyoke College, South Hadley, Massachusetts 01075, USA
⁵⁰Università di Napoli Federico II, Dipartimento di Scienze Fisiche and INFN, I-80126, Napoli, Italy
⁵¹NIKHEF, National Institute for Nuclear Physics and High Energy Physics, NL-1009 DB Amsterdam, The Netherlands
⁵²University of Notre Dame, Notre Dame, Indiana 46556, USA
⁵³Ohio State University, Columbus, Ohio 43210, USA
⁵⁴University of Oregon, Eugene, Oregon 97403, USA
⁵⁵Università di Padova, Dipartimento di Fisica and INFN, I-35131 Padova, Italy
⁵⁶Universités Paris VI et VII, Laboratoire de Physique Nucléaire et de Hautes Energies, F-75252 Paris, France
⁵⁷University of Pennsylvania, Philadelphia, Pennsylvania 19104, USA
⁵⁸Università di Perugia, Dipartimento di Fisica and INFN, I-06100 Perugia, Italy
⁵⁹Università di Pisa, Dipartimento di Fisica, Scuola Normale Superiore and INFN, I-56127 Pisa, Italy
⁶⁰Prairie View A&M University, Prairie View, Texas 77446, USA
⁶¹Princeton University, Princeton, New Jersey 08544, USA
⁶²Università di Roma La Sapienza, Dipartimento di Fisica and INFN, I-00185 Roma, Italy
⁶³Universität Rostock, D-18051 Rostock, Germany
⁶⁴Rutherford Appleton Laboratory, Chilton, Didcot, Oxon, OX11 0QX, United Kingdom
⁶⁵DSM/Dapnia, CEA/Saclay, F-91191 Gif-sur-Yvette, France
⁶⁶University of South Carolina, Columbia, South Carolina 29208, USA
⁶⁷Stanford Linear Accelerator Center, Stanford, California 94309, USA
⁶⁸Stanford University, Stanford, California 94305-4060, USA
⁶⁹State University of New York, Albany, New York 12222, USA
⁷⁰University of Tennessee, Knoxville, Tennessee 37996, USA
⁷¹University of Texas at Austin, Austin, Texas 78712, USA
⁷²University of Texas at Dallas, Richardson, Texas 75083, USA
⁷³Università di Torino, Dipartimento di Fisica Sperimentale and INFN, I-10125 Torino, Italy
⁷⁴Università di Trieste, Dipartimento di Fisica and INFN, I-34127 Trieste, Italy
⁷⁵IFIC, Universitat de Valencia-CSIC, E-46071 Valencia, Spain
⁷⁶Vanderbilt University, Nashville, Tennessee 37235, USA
⁷⁷University of Victoria, Victoria, British Columbia, Canada V8W 3P6
⁷⁸Department of Physics, University of Warwick, Coventry CV4 7AL, United Kingdom
⁷⁹University of Wisconsin, Madison, Wisconsin 53706, USA
⁸⁰Yale University, New Haven, Connecticut 06511, USA

(Dated: August 4, 2018)

A search for lepton-flavor and lepton-number violation in the decay of the tau lepton into one charged lepton and two charged hadrons is performed using 221.4 fb^{-1} of data collected at an e^+e^- center-of-mass energy of 10.58 GeV with the *BABAR* detector at the PEP-II storage ring. In all 14 decay modes considered, the observed data are compatible with background expectations, and upper limits are set in the range $\mathcal{B}(\tau \rightarrow \ell hh') < (0.7 - 4.8) \times 10^{-7}$ at 90% confidence level.

PACS numbers: 13.35.Dx, 14.60.Fg, 11.30.Hv, 11.30.Fs

Lepton-flavor violation (LFV) involving charged leptons has never been observed, and there are stringent experimental limits from muon decays: $\mathcal{B}(\mu \rightarrow e\gamma) < 1.2 \times 10^{-11}$ [1] and $\mathcal{B}(\mu \rightarrow eee) < 1.0 \times 10^{-12}$ [2] at 90% confidence level (CL). In tau decays, the most stringent limits on LFV are $\mathcal{B}(\tau \rightarrow \mu\gamma) < 6.8 \times 10^{-8}$ and $\mathcal{B}(\tau \rightarrow \ell\ell\ell) < (1 - 3) \times 10^{-7}$ at 90% CL [3, 4]. While forbidden in the Standard Model (SM), many extensions to the SM predict enhanced LFV in tau decays with respect to muon decays with branching fractions from 10^{-10} up to the current experimental limits [5]. Observation of LFV in tau decays would be a clear signature of physics beyond the SM, while non-observation will provide further constraints on theoretical models.

This paper presents the results of a search for lepton-flavor violation in the neutrinoless decays $\tau^- \rightarrow \ell^- h^+ h^-$ where ℓ represents an electron or muon and h represents a pion or kaon [6]. In addition, a search is also performed for the decays $\tau^- \rightarrow \ell^+ h^- h^-$ which also violate lepton-number conservation. All possible lepton and hadron combinations consistent with charge conservation are considered, leading to 14 distinct decay modes as shown in Table I. The best existing limits on the branching fractions for these decay modes currently come from CLEO: $(2 - 8) \times 10^{-6}$ at 90% CL [7].

The data used in this analysis were collected with the *BABAR* detector at the PEP-II asymmetric-energy e^+e^- storage ring. The data sample consists of 221.4 fb^{-1} recorded at a luminosity-weighted center-of-mass energy $\sqrt{s} = 10.58 \text{ GeV}$. With an estimated cross section for tau pairs of $\sigma_{\tau\tau} = (0.89 \pm 0.02) \text{ nb}$ [8], this data sample contains over 390 million tau decays.

Charged-particle (track) momenta are measured with a 5-layer double-sided silicon vertex tracker and a 40-layer drift chamber inside a 1.5-T superconducting solenoidal magnet. An electromagnetic calorimeter (EMC) consisting of 6580 CsI(Tl) crystals is used to identify electrons and photons, a ring-imaging Cherenkov detector (DIRC) and energy loss in the tracking system are used to identify charged hadrons, and the instrumented magnetic flux return (IFR) is used to identify muons. Further details on the *BABAR* detector are found in Ref. [9].

A Monte Carlo (MC) simulation of neutrinoless tau decays is used to study the performance of this analysis. Simulated $\tau^+\tau^-$ events including higher-order radiative corrections are generated using the KK2f MC generator [8], with one tau decaying to one lepton and two hadrons with a 3-body phase space distribution, while the second

tau decay is simulated with TAUOLA [10] according to measured rates [11]. Final state radiative effects are simulated for all decays using PHOTOS [12]. The detector response is simulated with GEANT [13], and the simulated events are reconstructed in the same manner as data.

Candidate signal events are required to have a 1-3 topology, where one tau decay yields one charged particle (1-prong), while the other tau decay yields three charged particles (3-prong). Four well reconstructed tracks are required with zero net charge, originating from a common region consistent with $\tau\tau$ production and decay. Pairs of oppositely charged tracks, likely to be from photon conversions in the detector material, are ignored if their e^+e^- invariant mass is less than $30 \text{ MeV}/c^2$. The event is divided into hemispheres using the plane perpendicular to the thrust axis, calculated from the observed track momenta and EMC energy deposits, in the center-of-mass (CM) frame. One hemisphere must contain exactly one track while the other must contain exactly three.

One of the charged particles found in the 3-prong hemisphere must be identified as either an electron or muon candidate. Electrons are identified using the ratio of observed EMC energy to track momentum (E/p), the shape of the shower in the EMC, and the ionization loss in the tracking system (dE/dx). Muons are identified by hits in the IFR and small energy deposits in the EMC. Each of the other two charged particles found in the 3-prong hemisphere must be identified as either a pion or a kaon, using information from the DIRC and dE/dx .

After event topology and particle identification requirements, there are significant backgrounds from light quark $q\bar{q}$ production and SM $\tau\tau$ events (without LFV), as well as small contributions from Bhabha, $\mu^+\mu^-$, and two-photon production of four charged particles. Additional selection criteria, largely the same for all 14 signal channels, are applied as follows. No photon candidates, identified as EMC energy deposits unassociated to a track, with $E_\gamma > 100 \text{ MeV}$ are allowed. This restriction removes $q\bar{q}$ backgrounds and SM $\tau\tau$ events. The total transverse momentum of the event in the CM frame must be greater than $0.2 \text{ GeV}/c$, while the polar angle of the missing momentum in the lab frame is required to be in the range $[0.25, 2.4]$ radians. These two requirements are effective at reducing two-photon and Bhabha backgrounds. The mass of the 1-prong hemisphere calculated from the four-momentum of the track in the 1-prong hemisphere and the missing momentum in the event, is required to be in the range $[0.6, 1.9] \text{ GeV}/c^2$ for ehh' candidates and

[0.8, 1.9] GeV/c^2 for $\mu hh'$ candidates. The 1-prong mass requirement is particularly effective at removing $q\bar{q}$ backgrounds as well as the remaining two-photon contribution. To reduce Bhabha backgrounds, the momentum of the 1-prong track in the CM frame is required to be less than 4.5 GeV/c for the $e\pi\pi$ candidates. In addition, particle identification vetoes are applied to specific selection channels. For all decay modes, lepton and pion candidates must not pass the kaon identification as well. For the ehh' decay modes, except for eKK , the 1-prong track must not be identified as an electron. This requirement is useful to reduce possible contamination from Bhabhas.

To further reduce backgrounds, candidate signal events are required to have an invariant mass and total energy in the 3-prong hemisphere consistent with the neutrinoless decay of a tau lepton. These quantities are calculated from the observed track momenta assuming the corresponding lepton and hadron masses for each decay mode. The mass difference and energy difference are defined as $\Delta M \equiv M_{\text{rec}} - m_\tau$ and $\Delta E \equiv E_{\text{rec}}^{\text{CM}} - E_{\text{beam}}^{\text{CM}}$, where M_{rec} is the reconstructed 3-prong invariant mass, $m_\tau = 1.777 \text{ GeV}/c^2$ is the tau mass [14], $E_{\text{rec}}^{\text{CM}}$ is the reconstructed 3-prong total energy in the CM frame, and $E_{\text{beam}}^{\text{CM}}$ is the CM beam energy. Rectangular signal regions are defined separately for each decay mode in the $(\Delta M, \Delta E)$ plane. For the $\mu hh'$ modes, ΔM is required to be in the range $[-20, +20] \text{ MeV}/c^2$, while for the ehh' modes the range is $[-30, +20] \text{ MeV}/c^2$ to account for radiative losses. For all 14 decay modes, ΔE must be in the range $[-100, +50] \text{ MeV}$.

These signal region boundaries are optimized to provide the smallest expected upper limits on the branching fractions in the background-only hypothesis. These expected upper limits are estimated using only MC simulations, not candidate events in data. To avoid bias, a blind analysis procedure was adopted with the number of data events in the signal region remaining unknown until the selection criteria were finalized and all systematic studies had been performed. Fig. 1 shows the observed data for all 14 selection channels, along with the signal region boundaries and the expected signal distributions.

The dominant remaining backgrounds are low multiplicity $q\bar{q}$ events and SM $\tau\tau$ events. These background classes have unique distributions in the $(\Delta M, \Delta E)$ plane: $q\bar{q}$ events populate the plane uniformly, while $\tau\tau$ backgrounds are restricted to negative values of both ΔM and ΔE . Backgrounds from Bhabha, $\mu\mu$, and two-photon events are found to be negligible. For each background class, a probability density function (PDF) describing the shape of the background distribution in the $(\Delta M, \Delta E)$ plane is determined by fitting an analytic function to the Monte Carlo prediction as described in more detail below. These PDFs are then combined with normalization coefficients determined from an unbinned maximum likelihood fit to the observed data in the $(\Delta M, \Delta E)$ plane in a sideband (SB) region. The resulting function describes the

TABLE I: Efficiency estimates, the number of expected background events (N_{bgd}) in the signal region (with total uncertainties), the number of observed events (N_{obs}) in the signal region, and the 90% CL upper limit for each decay mode.

Mode	Efficiency [%]	N_{bgd}	N_{obs}	UL at 90% CL
$e^- K^+ K^-$	3.77 ± 0.16	0.22 ± 0.06	0	$1.4 \cdot 10^{-7}$
$e^- K^+ \pi^-$	3.08 ± 0.13	0.32 ± 0.08	0	$1.7 \cdot 10^{-7}$
$e^- \pi^+ K^-$	3.10 ± 0.13	0.14 ± 0.06	1	$3.2 \cdot 10^{-7}$
$e^- \pi^+ \pi^-$	3.30 ± 0.15	0.81 ± 0.13	0	$1.2 \cdot 10^{-7}$
$\mu^- K^+ K^-$	2.16 ± 0.12	0.24 ± 0.07	0	$2.5 \cdot 10^{-7}$
$\mu^- K^+ \pi^-$	2.97 ± 0.16	1.67 ± 0.29	2	$3.2 \cdot 10^{-7}$
$\mu^- \pi^+ K^-$	2.87 ± 0.16	1.04 ± 0.18	1	$2.6 \cdot 10^{-7}$
$\mu^- \pi^+ \pi^-$	3.40 ± 0.19	2.99 ± 0.41	3	$2.9 \cdot 10^{-7}$
$e^+ K^- K^-$	3.85 ± 0.16	0.04 ± 0.04	0	$1.5 \cdot 10^{-7}$
$e^+ K^- \pi^-$	3.19 ± 0.14	0.16 ± 0.06	0	$1.8 \cdot 10^{-7}$
$e^+ \pi^- \pi^-$	3.40 ± 0.15	0.41 ± 0.10	1	$2.7 \cdot 10^{-7}$
$\mu^+ K^- K^-$	2.06 ± 0.11	0.07 ± 0.10	1	$4.8 \cdot 10^{-7}$
$\mu^+ K^- \pi^-$	2.85 ± 0.16	1.54 ± 0.25	1	$2.2 \cdot 10^{-7}$
$\mu^+ \pi^- \pi^-$	3.30 ± 0.18	1.46 ± 0.27	0	$0.7 \cdot 10^{-7}$

event rate observed in the SB region and is used to predict the expected background rate in the signal region. The SB region is defined as the rectangle, excluding the signal region, bounding ΔM in the range $[-0.7, +0.4] \text{ GeV}/c^2$ for ehh' final states and $[-0.4, +0.4] \text{ GeV}/c^2$ for $\mu hh'$ final states, while ΔE must be in the range $[-0.7, +0.4] \text{ GeV}$. The PDF shape determinations and SB fits are performed separately for each of the 14 decay modes.

For the $q\bar{q}$ backgrounds, a PDF is constructed from the product of two functions $P_{M'}$ and $P_{E'}$, where the coordinates $(\Delta M', \Delta E')$ have been rotated slightly from $(\Delta M, \Delta E)$ to better fit the expected distributions. The function $P_{M'}(\Delta M')$ is a Gaussian and the function $P_{E'}(\Delta E') = (1 - x/\sqrt{1+x^2})(1 + a_1x + a_2x^2 + a_3x^3)$ where $x = (\Delta E' - a_4)/a_5$ and a_i are fit parameters. The resulting $q\bar{q}$ PDF is described by eight fit parameters, including the rotation angle, which are determined by fits to MC $q\bar{q}$ background samples for each decay mode. For the $\tau\tau$ PDF, the function $P_{M'}(\Delta M')$ is the sum of two Gaussians with different widths above and below the peak, while the functional form of $P_{E'}(\Delta E')$ is the same as the $q\bar{q}$ PDF above. To properly model the wedge-shaped kinematic limit in tau decays, a coordinate transformation of the form $\Delta M' = \cos \beta_1 \Delta M + \sin \beta_1 \Delta E$ and $\Delta E' = \cos \beta_2 \Delta E - \sin \beta_2 \Delta M$ is performed. In total there are 12 free parameters describing this PDF, and all are determined by fits to MC $\tau\tau$ samples.

With the shapes of the two background PDFs determined, an unbinned maximum likelihood fit to the data in the SB region is used to find the expected rate of each background type in the signal region. Extensive MC studies show that these PDF functions adequately describe the predicted background shapes near the signal regions. The accuracy of these predictions is verified by comparing to data in regions neighboring the signal re-

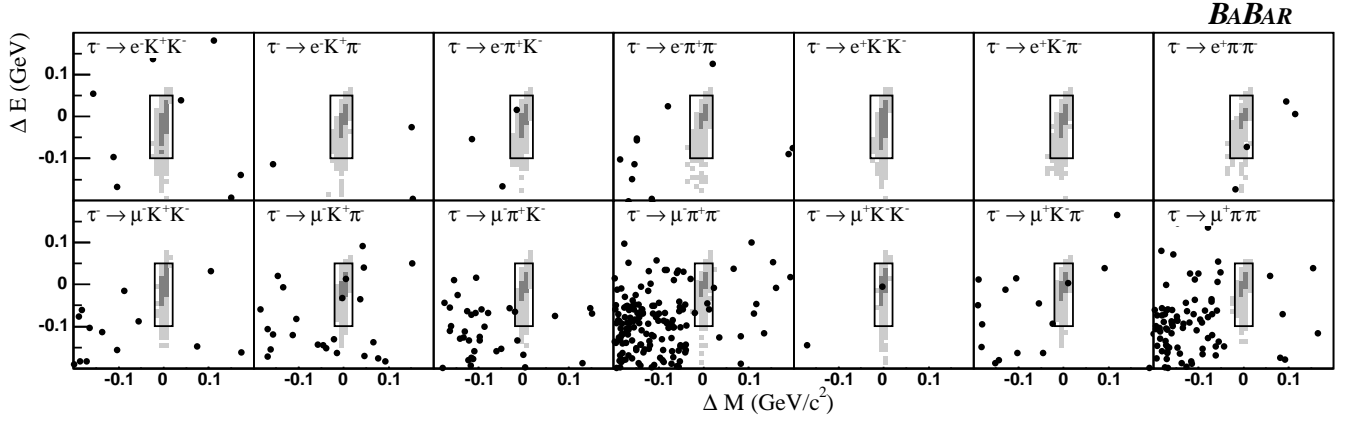


FIG. 1: Observed data shown as dots in the $(\Delta M, \Delta E)$ plane and the boundaries of the signal region for each decay mode. The dark and light shading indicates contours containing 50% and 90% of the selected MC signal events, respectively.

gion in the $(\Delta M, \Delta E)$ plane where no signal is expected. Expected backgrounds are shown in Table I, and an example of the background prediction compared to the observed data is shown in Fig. 2.

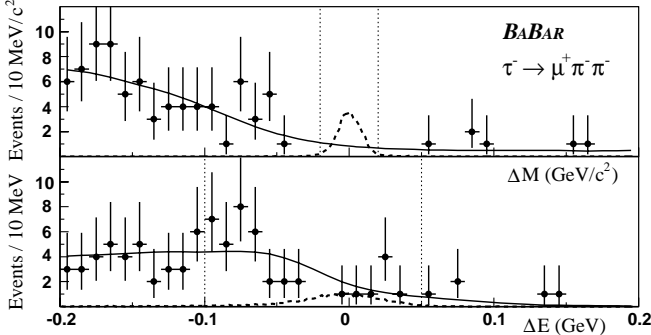


FIG. 2: Data (points) and background expectation (solid line) are shown for the $\mu^+\pi^-\pi^-$ candidates displayed in Fig. 1. Expected signal distributions for a branching fraction of 5×10^{-7} are also shown as the dashed curve. The vertical lines indicate the signal region.

The efficiency of the selection for signal events is estimated with a MC simulation of neutrinoless tau decays. About 40% of the MC signal events pass the initial 1-3 topology requirement, and 20% to 70% of these pre-selected events pass the particle identification (PID) criteria, depending upon the signal mode. The final efficiency for signal events to be found in the signal region after all requirements is shown in Table I for each decay mode and ranges from 2.1% to 3.8%. This efficiency includes the 85% branching fraction for 1-prong tau decays [11].

The PID selection efficiencies and misidentification rates are measured directly using tracks in kinematically-selected data control samples. These values are parameterized as a function of particle momentum, charge, polar angle, and azimuthal angle in the laboratory frame. The lepton-identification criteria have been designed to give

very low mis-identification rates at the expense of some efficiency loss. The electron ID is expected to be 81% efficient in signal ehh' events, with a mis-ID rate of 0.1% for pions and 0.2% for kaons in generic $\tau\tau$ events. The muon ID is 44% efficient for $\mu hh'$ signal events, with a mis-ID rate of 1.0% for pions and 0.4% for kaons. The hadronic identification is designed to classify the hadronic candidates as pions or kaons, but is not intended to distinguish hadrons from leptons. The pion ID is 92% efficient with a mis-ID rate of 12% for kaons, while the kaon ID is 81% efficient with a 1.4% mis-ID rate for pions.

The largest systematic uncertainty for the signal efficiency is the uncertainty in measuring particle ID efficiencies. This uncertainty (all uncertainties quoted are relative) is dominated by the statistical precision of the PID control samples, and ranges from 0.7% for $e^-\pi^+\pi^-$ to 3.8% for $\mu^-K^+K^-$. The modeling of the tracking efficiency contributes an uncertainty of 2.5%, while the restriction on extra photons leads to an additional uncertainty of 2.4%. All other sources of uncertainty are found to be small, including the modeling of radiative effects, track momentum resolution, trigger performance, observables used in the selection criteria, and knowledge of the tau 1-prong branching fractions. No uncertainty is assigned for possible model dependence of the signal decay. The selection efficiency is found to be uniform within 20% across the Dalitz plane, provided the invariant mass for any pair of particles is less than $1.4 \text{ GeV}/c^2$.

Since the background levels are extracted directly from the data, systematic uncertainties on the background estimation are directly related to the background normalization, parameterization, and the fit technique used. The finite data available in the SB region used to determine the background rates dominates the background uncertainty. Additional uncertainties of 10% are estimated by varying the fit procedure and changing the functional form of the background PDFs. The uncertainty on the branching fraction of SM tau decays with one or two

kaons is also evaluated, and contributes less than 15% for all final states.

The numbers of events observed (N_{obs}) and the background expectations (N_{bgd}) are shown in Table I, with no significant excess observed. Upper limits on the branching fractions are calculated according to $\mathcal{B}_{UL}^{90} = N_{UL}^{90}/(2\varepsilon L\sigma_{\tau\tau})$, where N_{UL}^{90} is the 90% CL upper limit for the number of signal events when N_{obs} events are observed with N_{bgd} background events expected. The quantities ε , L , and $\sigma_{\tau\tau}$ are the selection efficiency, luminosity, and $\tau^+\tau^-$ cross section, respectively. The branching fraction upper limits are calculated including all uncertainties using the technique of Cousins and Highland [15] following the implementation of Barlow [16]. The estimates of L and $\sigma_{\tau\tau}$ are correlated [17], and the uncertainty on the product $L\sigma_{\tau\tau}$ is 2.3%. The 90% CL upper limits on the $\tau \rightarrow \ell hh'$ branching fractions, shown in Table I, are in the range $(0.7 - 4.8) \times 10^{-7}$. These limits represent an order of magnitude improvement over the previous experimental bounds [7].

We are grateful for the excellent luminosity and machine conditions provided by our PEP-II colleagues, and for the substantial dedicated effort from the computing organizations that support *BABAR*. The collaborating institutions wish to thank SLAC for its support and kind hospitality. This work is supported by DOE and NSF (USA), NSERC (Canada), IHEP (China), CEA and CNRS-IN2P3 (France), BMBF and DFG (Germany), INFN (Italy), FOM (The Netherlands), NFR (Norway), MIST (Russia), and PPARC (United Kingdom). Individuals have received support from CONACyT (Mexico), A. P. Sloan Foundation, Research Corporation, and Alexander von Humboldt Foundation.

[†] Also with Università della Basilicata, Potenza, Italy

[‡] Deceased

- [1] MEGA/LAMPF Collaboration, M. L. Brooks *et al.*, Phys. Rev. Lett. **83**, 1521 (1999).
- [2] SINDRUM Collaboration, U. Bellgardt *et al.*, Nucl. Phys. B **299**, 1 (1988).
- [3] *BABAR* Collaboration, B. Aubert *et al.*, SLAC-PUB-11028, submitted to *Phys. Rev. Lett.*
- [4] *BABAR* Collaboration, B. Aubert *et al.*, Phys. Rev. Lett. **92**, 121801 (2004).
- [5] E. Ma, Nucl. Phys. B Proc. Suppl. **123**, 125 (2003).
- [6] Throughout this paper, charge conjugate decay modes also are implied.
- [7] CLEO Collaboration, D. W. Bliss *et al.*, Phys. Rev. D **57**, 5903 (1998).
- [8] B. F. Ward, S. Jadach, and Z. Was, Nucl. Phys. Proc. Suppl. **116**, 73 (2003).
- [9] *BABAR* Collaboration, B. Aubert *et al.*, Nucl. Instr. Methods Phys. Res., Sect. A **479**, 1 (2002).
- [10] S. Jadach, Z. Was, R. Decker, and J. H. Kuhn, Comput. Phys. Commun. **76**, 361 (1993).
- [11] Particle Data Group, S. Eidelman *et al.*, Phys. Lett. **B592**, 1 (2004).
- [12] E. Barberio and Z. Was, Comput. Phys. Commun. **79**, 291 (1994).
- [13] GEANT4 Collaboration, S. Agostinelli *et al.*, Nucl. Instr. Methods Phys. Res., Sect. A **506**, 250 (2003).
- [14] BES Collaboration, J. Z. Bai *et al.*, Phys. Rev. D **53**, 20 (1996).
- [15] R. D. Cousins and V. L. Highland, Nucl. Instr. Methods Phys. Res., Sect. A **320**, 331 (1992).
- [16] R. Barlow, Comput. Phys. Commun. **149**, 97 (2002).
- [17] The luminosity is measured using the observed $\mu^+\mu^-$ rate, and the $\mu^+\mu^-$ and $\tau^+\tau^-$ cross sections are both estimated with KK2f.

* Also with Università di Perugia, Dipartimento di Fisica, Perugia, Italy